*2536–2549* *Nucleic Acids Research, 2006, Vol. 34, No. 9*
*doi:10.1093/nar/gkl286*

# G-quadruplex formation within the promoter of the *KRAS* proto-oncogene and its effect on transcription

**Susanna Cogoi and Luigi E. Xodo***

Department of Biomedical Science and Technology, School of Medicine, P.le Kolbe 4, 33100 Udine, Italy

Received February 7, 2006; Revised March 7, 2006; Accepted April 5, 2006

## ABSTRACT

**In human and mouse, the promoter of the *KRAS* gene contains a nuclease hypersensitive polypurine–polypyrimidine element (NHPPE) that is essential for transcription. An interesting feature of the polypurine G-rich strand of NHPPE is its ability to assume an unusual DNA structure that, according to circular dichroism (CD) and DMS footprinting experiments, is attributed to an intramolecular parallel G-quadruplex, consisting of three G-tetrads and three loops. The human and mouse *KRAS* NHPPE G-rich strands display melting temperature of 64 and 73°C, respectively, as well as a $K^+$-dependent capacity to arrest DNA polymerase. Photocleavage and CD experiments showed that the cationic porphyrin TMPyP4 stacks to the external G-tetrads of the *KRAS* quadruplexes, increasing the $T_m$ by ~20°C. These findings raise the intriguing question that the G-quadruplex formed within the NHPPE of *KRAS* may be involved in the regulation of transcription. Indeed, transfection experiments showed that the activity of the mouse *KRAS* promoter is reduced to 20% of control, in the presence of the quadruplex-stabilizing TMPyP4. In addition, we found that G-rich oligonucleotides mimicking the *KRAS* quadruplex, but not the corresponding 4-base mutant sequences or oligonucleotides forming quadruplexes with different structures, competed with the NHPPE duplex for binding to nuclear proteins. When vector pKRS-413, containing CAT driven by the mouse *KRAS* promoter, and *KRAS* quadruplex oligonucleotides were co-transfected in 293 cells, the expression of CAT was found to be down-regulated to 40% of the control. On the basis of these data, we propose that the NHPPE of *KRAS* exists in equilibrium between a double-stranded form favouring transcription and a folded quadruplex form, which instead inhibits transcription. Such a mechanism, which is probably adopted by other growth-related genes, provides useful hints for the rational design of anticancer drugs against the *KRAS* oncogene.**

## INTRODUCTION

Pancreatic ductal adenocarcinoma is an aggressive disease, which is characterized by a rapid progression and little response to conventional cancer treatments (1). Like many other tumours, pancreatic cancer results from the accumulation of genetic lesions in various genes: proto-oncogenes, tumour-suppression and maintenance genes (2,3). The *KRAS* gene is located in chromosome 12, locus 12p12.1, and encodes for a 21 kDa protein, $p21^{RAS}$, which is anchored to the inner surface of the plasma membrane and acts as a molecular switch that transmits to the nucleus, through the Raf-MAP kinase pathway, signals that influence cell growth and apoptosis (4). Protein $p21^{RAS}$ exists in two states, a GTP-bound active state and a GDP-bound inactive state. The activity of $p21^{RAS}$ is regulated positively by nucleotide exchange factors and negatively by a GTPase activating protein. When there is a point mutation in codon 12 (5), the protein is locked in the active state and constitutively transmits to the nucleus mitogenic signals. In a recent work, Hingorani *et al*. (6) have investigated the role of oncogenic RAS mutations in the pancreatic tumorigenesis. They demonstrated that the endogenous expression of an oncogenic *KRAS* allele ($KRAS^{G12D}$) in mouse pancreas initiates the development of pancreatic ductal adenocarcinoma in a way identical to that occurring in the cognate human condition. The rapid accumulation of knowledge on the molecular biology of pancreatic adenocarcinoma has stimulated the development of targeted therapies for this disease. Strategies aiming at the suppression of *KRAS* expression (7–11) or inactivation of the Ras protein (12) have been proposed. In this context, we have addressed

*To whom correspondence should be addressed. Tel: +39 0432 494395; Fax: +39 0432 494301; Email: lxodo@makek.dstb.uniud.it

our efforts on a polypurine–polypyrimidine motif located in the *KRAS* promoter, between nt −327 and −296 in human; −318 and −290 in mouse (13,14). Polypurine–polypyrimidine motifs are simple repeats distributed through the eukaryotic genomes (15) and often are present in the 5′ region of the genes. The *CMYC* region between −142 and −115 from the P1 promoter which controls 80–90% of transcription (16), harbours a polypurine–polypyrimidine motif that extrudes a G-quadruplex structure involved in transcription regulation (17,18). In *Drosophila*, the 5′ region of *HSP26* and *HSP70* contains a polypurine–polypyrimidine stretch that binds to nuclear proteins and activates transcription (19). In the proximal promoter region of the human VEGF gene there is a *polypurine-polypyrimidine* sequence forming a G-quadruplex (20). In addition, other genes contain oligopurine tracts in the regulatory regions (e.g. c-fes/fps, c-ets-2, c-myb, c-src) (21–24). Studies on chromatin showed that the *KRAS* polypurine–polypyrimidine motif is a nuclease hypersensitive element (NHPPE), suggesting that it may adopt a non-B-DNA structure (13,14). NHPPE is essential for the promoter activity as its excision results in a significant downregulation of transcription (14). Owing to its critical role, we have previously targeted NHPPE with triplex-forming oligonucleotides (TFOs) (9). In the first approach we successfully targeted a reporter gene driven by the *KRAS* promoter. However, when the designed TFOs were used against endogenous *KRAS*, we did not obtain satisfactory results. We though that the TFO uptake might be a serious obstacle, thus we obtained from Panc-1 cells a stable transfectant line in which an anti-*KRAS* TFO was endogenously produced (10). In the transfectant line, we observed that oncogenic *KRAS* was downregulated and as a result cell proliferation and colony formation were strongly reduced, while apoptosis was enhanced. However, we believed that these cellular effects could not be ascribed to the formation of a triplex between the endogenous TFO and NHPPE, as *in vitro* experiments suggested that the RNA•DNA•DNA triplex was not stable enough to elicit such strong cellular effects. Interestingly, we found that the anti *KRAS* activity of the endogenous TFO correlated with its ability assume a G-quadruplex that recognises a nuclear protein binding to the NHPPE duplex (10,11). In the present work we report that the purine strand of NHPPE, located in the proximal promoter sequence of *KRAS*, is also able to form a G-quadruplex, suggesting that this unusual DNA structure may be involved in transcription. We have characterized the G-quadruplexes formed in the mouse and human promoters through electrophoretic mobility shift assay (EMSA), circular dichroism (CD), chemical probing with DMS/piperidine and polymerase stop assays. Transfection experiments showed that the stabilization of the *KRAS* G-quadruplex with the cationic porphyrin TMPyP4 results in a strong inhibition of *KRAS* transcription. Furthermore, DNA–protein competition assays showed that the mouse and human *KRAS* G-quadruplexes recognize a nuclear protein that binds to duplex NHPPE. The sequestration of this protein by an oligonucleotide mimicking the *KRAS* G-quadruplex, induced a transcription inhibition to 40% of control. Our data suggest a transcription mechanism that involves the formation of a G-quadruplex within the *KRAS* promoter and shed light on new molecular strategies to suppress the expression of *KRAS* in tumour cells.

## MATERIALS AND METHODS

### DNA samples

The oligonucleotides illustrated in Table 1 were obtained from Sigma-Proligo (Paris, France). The oligonucleotides were purified by electrophoresis using a denaturing 20% polyacrylamide gel (acrylamide:bisacrylamide, 19/1) in TBE, 7 M urea, 55°C. The bands were excised from the gel and eluted in water. The DNA solutions were filtered (Ultrafree-DA, Millipore) and precipitated. The concentration of each DNA was determined from the absorbance at 260 nm in milli Q water, using as extinction coefficients 7500, 8500, 15 000 and 12 500 $M^{-1}cm^{-1}$ for C, T, A and G, respectively. Plasmid pKRS-413 was a gift of D. L. George (University of Pennsylvania).

### Circular dichroism

CD spectra were obtained using a JASCO J-600 spectropolarimeter equipped with a thermostatted cell holder. The DNAs used in the CD experiments were at a concentration of 3 μM, in 50 mM Tris, pH 7.2 and 100 mM KCl. Spectra were recorded in 0.5 cm quartz cuvette. A thermometer inserted in the cuvette holder allowed a precise measurement of the sample temperature. The spectra were calculated with J-700 Standard Analysis software (Japan Spectroscopic Co., Ltd) and are reported as ellipticity (mdeg) versus wavelength (nm). Each spectrum was recorded three times, smoothed and subtracted to the baseline.

### Native gel electrophoresis

Oligonucleotides (5 nM) end-labelled with [γ-$^{32}$P]ATP (Amersham, Pharmacia-Biotech, Milan) and polynucleotide kinase were incubated for 3 h in the buffer as specified in the figure legends. After incubation, the samples were loaded on a 20% polyacrylamide (acrylamide: bisacrylamide, 19/1) non-denaturing TBE gel and run for 2.5 h at 20 W with temperature control at 25°C. The gels were fixed in 10% methanol, 10% acetic acid, dried and exposed to a Hyperfilm MP (Amersham) at −80°C for few hours.

### Preparation of nuclear extracts

Nuclear extracts were obtained as described by Dignam (25). Briefly, 10 × 10 cm plates of confluent Panc-1 or NIH 3T3 cells were collected and resuspended in hypotonic buffer. Swollen cells were homogenized with a Dounce and the nuclei, pelleted by centrifugation, were resuspended in low-salt buffer (20 mM HEPES, pH 7.9, 25% glycerol, 1.5 mM MgCl2, 0.02 M KCl, 0.2 mM EDTA, 0.2 mM phenylmethylsulfonyl fluoride and 0.5 mM

**Table 1.** Oligonucleotides used in this study

| | |
|---|---|
| 5′-GGGAGGGAGGGAAGGAGGGAGGGAGGGA | 28Rm |
| 5′-GGGAGCGAGCGAAGGAGGGAGCGAGCGA | 28Rmut |
| 5′-AGGGCGGTGTGGGAAGAGGGAAGAGGGGGAGG | 32Rh |
| 5′-AGCGCGGTGTGCGAAGAGCGAAGAGCGGGAGG | 32Rmut |
| 5′-TCCCTCCCTCCCTCCTTCCCTCCCTCCC | 28Ym |
| 5′-CCTCCCCCTCTTCCCTCTTCCCACACCGCCCT | 32Yh |
| 5′-UGGGGU | Q1 |
| 5′-GUUUUUGGGGCUUUUC | Q2 |
| 5′-TGGGGAGGGTGGGGAGGGTGGGGAAGG | CMYC |

DTT). Release of nuclear proteins was obtained by the addition of a high-salt buffer (as low-salt buffer but with 1.2 M KCl). Protein concentration was measured according to the Lowry method.

### DMS footprinting and photocleavage experiments

Purified oligonucleotides 32Rh, 32Rmut, 28Rm and 28Rmut (25 nM), end-labelled with [$\gamma$-$^{32}$P]ATP (Amersham) and polynucleotide kinase (New England Biolabs, MA), were incubated overnight at 37°C, in 50 mM sodium cacodylate, pH 8, 1 mM EDTA, 50 or 100 mM KCl, 1 μg sonicated salmon sperm DNA and 50 or 100 nM TMPyP4 as specified in figure legends. Dimethylsulphate (DMS) dissolved in ethanol (DMS:ethanol, 4/1, vol/vol) was added to the DNA solution (1 μl to a total volume of 70 μl) and left to react for 5 min at room temperature. For photocleavage experiments, the DNA solutions containing 100 nM TMPyP4 were incubated in cocodylate buffer containing 100 mM KCl, and treated for 30 min with a white light from a Solaris 2 (J615) projector (150 W) at a fluence rate of 64 mW/cm$^2$. Both DMS and Photocleavage reactions were stopped by the addition of 1:4 vol of Stop solution (1.5 M sodium acetate, pH 7, 1 M β-mercaptoethanol and 1 μg/μl tRNA). DNA was precipitated with 4 vol of ethanol and resuspended in piperidine 1 M. After cleavage at 90°C for 30 min, reactions were stopped with chilling in ice followed by precipitation with 0.3 M sodium acetate, pH 5.2 and 3 vol of ethanol. The DNA samples were resuspended in 90% formamide and 50 mM EDTA, denatured at 90°C and run for 2 h on a denaturing 20% polyacrylamide gel, prepared in TBE and 8 M urea, pre-equilibrated at 55°C in a Sequi-Gen GT Nucleic Acids Electrophoresis Apparatus (Bio-Rad, CA), which was equipped with a thermocouple that allows a precise temperature control. After running, the gel was fixed in a solution containing 10% acetic acid and 10% methanol, dried at 80°C and exposed to Hyperfilm MP (Amersham) for autoradiography.

### Polymerase stop assay

Plasmid pKRS-413 or *KRAS* single-stranded DNA templates were subjected to a denaturation/renaturation cycle by NaOH/HCl treatment. The treated DNAs (15 nM) were mixed with the primer for DNA polymerase (7.5 nM, see Figure 3), 100 mM KCl, 100 nM TMPyP4 and Klenow buffer (New England Biolabs). After 24 h of incubation at 45°C, the primer extention reactions were carried out in 30 min, by adding 10 mM DTT, 100 μM dATP, dGTP, dTTP, 1 μM [$\alpha$-$^{32}$P]dCTP (7.4 Bq) and 3.75 U DNA Polymerase I (large Klenow fragment) (New England BioLabs). The reactions were stopped by adding an equal volume of stop buffer (95% formamide, 10 mM EDTA, 10 mM NaOH, 0.1% xylene cyanol and 0.1% bromophenol blue). The products were separated on a 15% polyacrylamide sequencing gel prepared in TBE, 8 M urea. The gel was dried and exposed to autoradiography.

### EMSA

Protein–DNA interactions were analysed by mobility shift assays. End-labelled NHPPE duplexes (5 nM) were incubated in 20 mM Tris–HCl, pH 8, 30 mM KCl, 1.5 nM $MgCl_2$, 1 nM DTT, 8% glycerol, 1% Phosphatase Inhibitor Cocktail I (Sigma), 5 mM NaF, 1 mM $Na_3VO_4$, 25 nM poly(dIdC) and 0.25 ng/μl nuclear extract, for 2 h at 37°C.

### Southwestern blotting

An aliquot of 25 μg of nuclear protein extract were loaded in each lane and separated in 8% PAGE–SDS gel and electroblotted in 25 mM Tris, 192 mM Glycine, 20% methanol and 0.1% SDS on a nitrocellulose transfer membrane. Denaturation was performed with 6 M guanidine–HCl for 30 min at 4°C, followed by renaturation with increasing dilutions with HEPES-binding buffer (25 mM HEPES, pH 7.9, 4 mM KCl and 3 mM $MgCl_2$), 1:1, 1:2 and 1:4, each wash was carried out at 4°C for 15 min. The blotted membrane was treated for 1 h with 5% non-fat milk in HEPES-binding buffer. Hybridization with radiolabelled DNA was carried out in 0.5% non-fat dried milk, 1% NP40, 1 mg/ml poly(dIdC) in HEPES-binding buffer, 1000 c.p.m./ml of radiolabelled probe, which was preincubated in 50mM Tris–HCl, pH 7.4, 100 mM KCl for 2 h at 37°C.

### Cell cultures and transient transfections

Human transformed kidney 293 cells were cultured in DMEM, containing 100 U/ml penicillin, 100 μg/ml streptomycin, 200 mM L-glutamine and 10% foetal bovine serum (Celbio, Milan, Italy). Cells were maintained in logarithmic phase of growth. For transfection experiments, $6 \times 10^5$ cells were seeded in a 35 mm culture dish and treated for 24 h with TMPyP4 at different concentrations (3–15 μM). Each plate was co-transfected with 2 μg of pKRS-413 and 50 ng of pTK β-gal with calcium phosphate method. After 48 h, ELISA assays were performed with CAT and β-gal ELISA kits (Roche Diagnostics, Milan, Italy) as manufacturer's instructions. Samples were read at 405 nm with reference filter at 490 nm with an Ultra Microplate Reader (Bio-Tek Instruments, INC) with a kinetic reading for 40 min. Oligonucleotides were transfected with Lipofectamine 2000 (Invitrogen) following manufacturer protocol 8 h before plasmid transfection.

## RESULTS

### The purine strands of human and mouse *polypurine-polypyrimidine's* form G-quadruplex structures

The promoter of the *KRAS* gene contains a nuclease hypersensitive polypurine–polypyrimidine element upstream from the major transcription initiation site (13,14). This sequence is located between nt −318/−290 in mouse (Accession no. M16708), −327/−296 in human (Accession no. L00044), positions relative to the exon 0/intron 1 boundary. Previous studies have shown that NHPPE is bound by nuclear proteins and plays an essential role in transcription (14). The NHPPE sequences are highly conserved in mouse and human and characterized by a high C+G content (72% mouse, 67% human) (Figure 1). Here, we asked whether the G-rich strands of the NHPPEs adopt a non-B-DNA structure. Since G-rich oligonucleotides can form quadruplex structures in KCl (26), we analysed by CD the purine strands of the mouse and human NHPPEs, namely 28Rm and 32Rh, and the corresponding

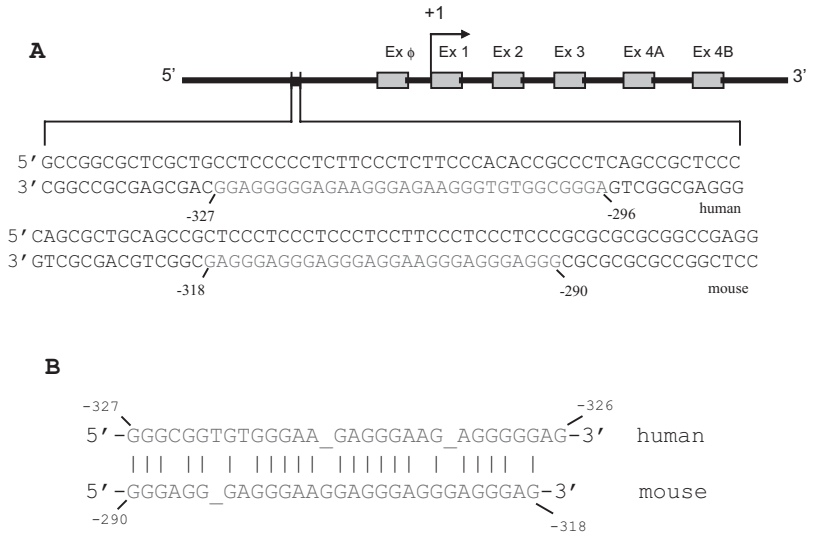


**Figure 1.** (**A**) Sequences of the NHPPEs contained in the human and mouse *KRAS* genes. Positions relative to exon 0/intron 1 boundary are shown. (**B**) Human and mouse NHPPEs show a high sequence homology.

4-base mutant sequences, 28Rmut and 32Rmut, in 50 mM Tris–HCl, pH 7.4 and 100 mM KCl. Figure 2A shows that both 32Rh and 28Rm exhibit a CD spectrum characterized by a strong and positive ellipticity at 260 nm and a weaker and negative ellipticity at 240 nm. This spectrum is similar to those reported for oligonucleotides that are known to assume a parallel quadruplex structure, d(TGGGGT) (27,28) and d(GGA)$_4$ (29). Interestingly, the CD spectra of the 4-base mutants 28Rmut and 32Rmut, in which the central guanine in four runs of guanines (Table 1) has been replaced with cytosine, appear dramatically different and not consistent with a quadruplex structure. Another evidence that the *KRAS* G-rich sequences form a G-quadruplex structure was obtained by UV thermal difference spectra (TDS), as they provide a distinctive spectroscopic signature for G-quadruplex formation (30,31). We have, measured the TDS spectra of 32Rh, 28Rm and, for comparison, of the *CMYC* sequence (Table 1), that is known to form a parallel quadruplex (32,33). The spectra obtained (Supplementary Figures S1 and S2) show the typical features of quadruplex DNA, with negative minima at 262 and 295 nm, positive maxima at 255 and 270, a shoulder at 245 nm (30,31). To determine the stability of the putative parallel G-quadruplexes formed by 28Rm and 32Rh, we measured the CD spectra as a function of temperature and plotted the ellipticity at 260 nm versus temperature. We obtained two melting curves showing that the human and mouse G-quadruplexes denatured in a cooperative way with $T_m$'s of 64 and 73°C, respectively (data not shown). We then wondered whether the parallel quadruplexes formed by the two *KRAS* promoter sequences are intra- or intermolecular. To answer this question, we analysed the electrophoretic mobilities of 28Rm, 32Rh, 28Rmut and 32Rmut, under native conditions (Figure 2B). The wild-type sequences (5 nM), incubated either in NaCl or KCl, migrated in a 20% polyacrylamide gel much faster than the corresponding duplexes. The mobility appeared only slightly slower than the complementary pyrimidine strands or 4-base mutants, which migrate as single-stranded species. This suggests that both 28Rm and 32Rh adopt an intramolecular quadruplex structure. In fact, increasing 200-fold the oligonucleotide concentration from 5 nM to 1 μM, the mobility of the wild-type sequences does not change [lane 5 (mouse); lane 9 (human)]. In principle, both 28Rm and 32Rh could form G–G hairpins that associate into bimolecular quadruplexes. However, these quadruplexes should have a mobility not much different from that of the duplex; for instance $TAG_3T$-$TAG_3T$, whose crystal shows that it forms a parallel bimolecular quadruplex (34), migrates in much the same way as the duplex does (35). Finally, the observations that (i) the CD spectra of 28Rm and 32Rh do not change following a DNA dilution from 2 μM to 200 nM (data not shown), (ii) 28Rm and 32Rh after denaturing give rapidly the typical CD signature and electrophoretic mobility (lanes 6 and 7 mouse; lanes 5 and 6 human), argue strongly in favour of an intramolecular folding.

### *KRAS* G-quadruplex arrests DNA polymerase

It has been shown that G-quadruplex structures are able to block primer extension by DNA polymerase in a $K^+$-dependent manner (36,37). We therefore designed four DNA templates—two containing the mouse and human wild-type G-rich sequences, two containing the 4-base mutant sequences—and analysed their capacity to form an intramolecular G-quadruplex by a DNA polymerase arrest assay. Figure 3 shows the results of primer extension experiments performed with the mouse templates at 37°C, in the presence of NaCl, KCl or KCl+TMPyP4 (tetra-(*N*-methyl-4-pyridil porphyrin), a cationic porphyrin that stabilizes quadruplex DNA (38). In order to determine the exact point in which DNA polymerase was arrested, we sequenced the template by the Sanger (dideoxy) method (lanes 1–4). A potassium-dependent arrest of DNA polymerase at the adenine preceding the first run of guanines at the 3′ side of the G-rich sequence can be seen in lanes 6 and 7. This premature chain termination product appeared stronger in the presence

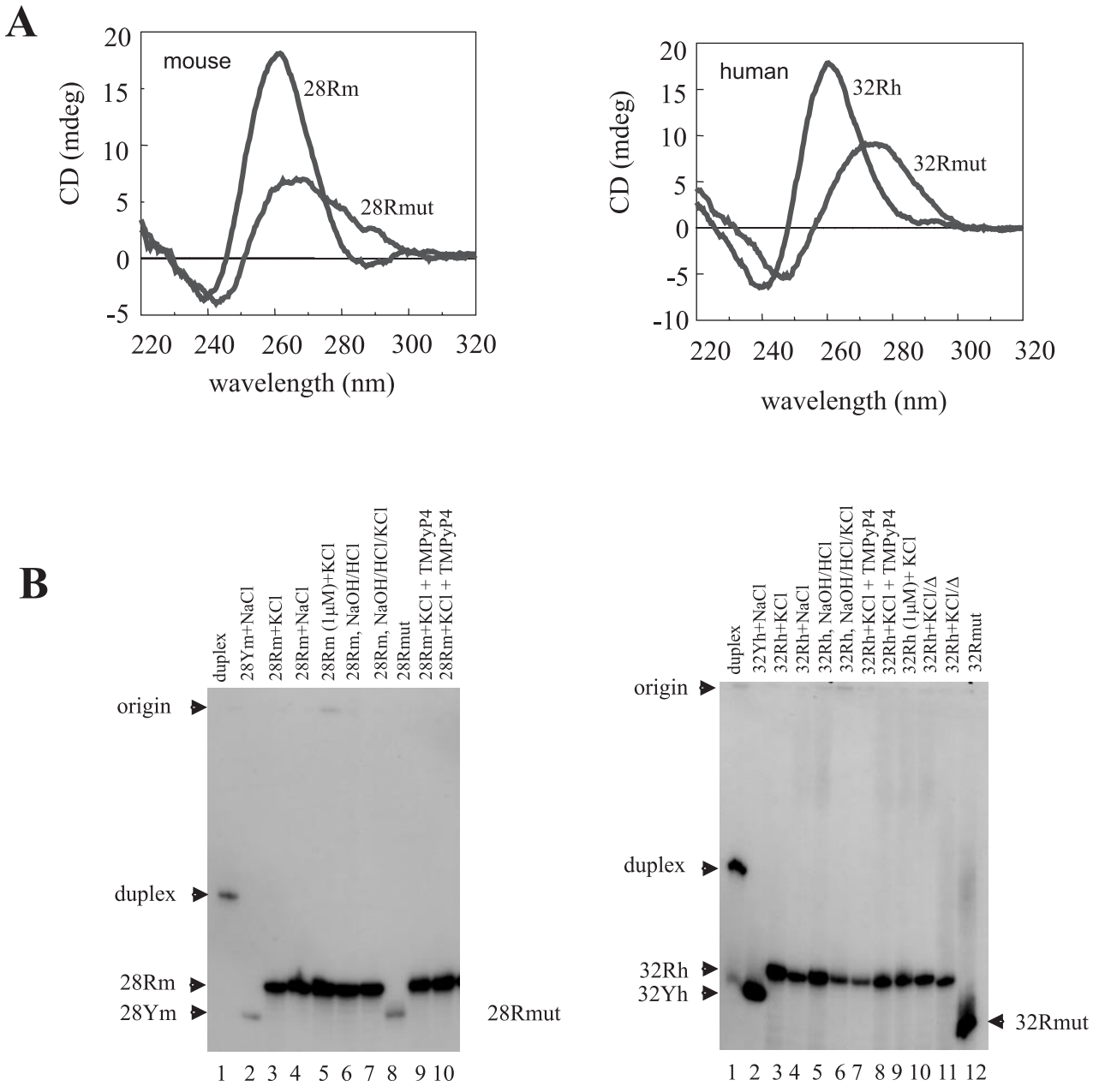


**Figure 2.** (**A**) CD spectra of the G-rich strands of the mouse (28Rm) and human (32Rh) NHPPEs and corresponding 4-base mutant sequences (28Rmut, 32Rmut). Spectra have been obtained in 50 mM Tris, pH 7.2, 100 mM KCl, oligonucleotide concentration 3 μM. (**B**) Native electrophoretic mobilities of the NHPPE duplexes, 28Rm, 32Rh, pyrimidine strands 28Ym and 32Yh, 28Rmut and 32Rmut under various experimental conditions. The oligonucleotides were radiolabelled, incubated for 5 h in the appropriate buffer and run at 25°C in a 20% polyacrylamide gel in TBE. Samples in lanes 6 and 7 (left panel) and 5 and 6 (right panel) were denatured with NaOH and renatured with HCl.

of the stabilizing ligand TMPyP4. In addition to the primary pausing site at the beginning of the G-rich motif, a secondary pausing site is observed at the adenine preceding the second run of guanines. This suggests the formation of an alternative G-quadruplex within the mouse G-rich motif, starting from the second 3′ G-run. Note that in the presence of NaCl, DNA polymerase was not arrested and produced a full length transcript (lane 5). It is noteworthy that when 4 guanines are replaced with cytosines, the polymerase was not arrested, indicating that the 4-base mutant sequence did not form a G-quadruplex, in accord with PAGE and CD (lanes 8–10). Next, we wondered whether the *KRAS* G-quadruplex can be extruded from a double-stranded template containing NHPPE. We performed primer extension experiments using as template plasmid pKRS-413, which contains the mouse *KRAS* promoter. We designed a primer complementary to a sequence located downstream from the G-rich motif, which was used for both DNA sequencing and primer extension reactions (Figure 4). It can be seen that DNA polymerase is arrested at the adenine preceding the first 3′ run of guanines, in perfect accord with the results obtained with the single-stranded template. The arrest of polymerase

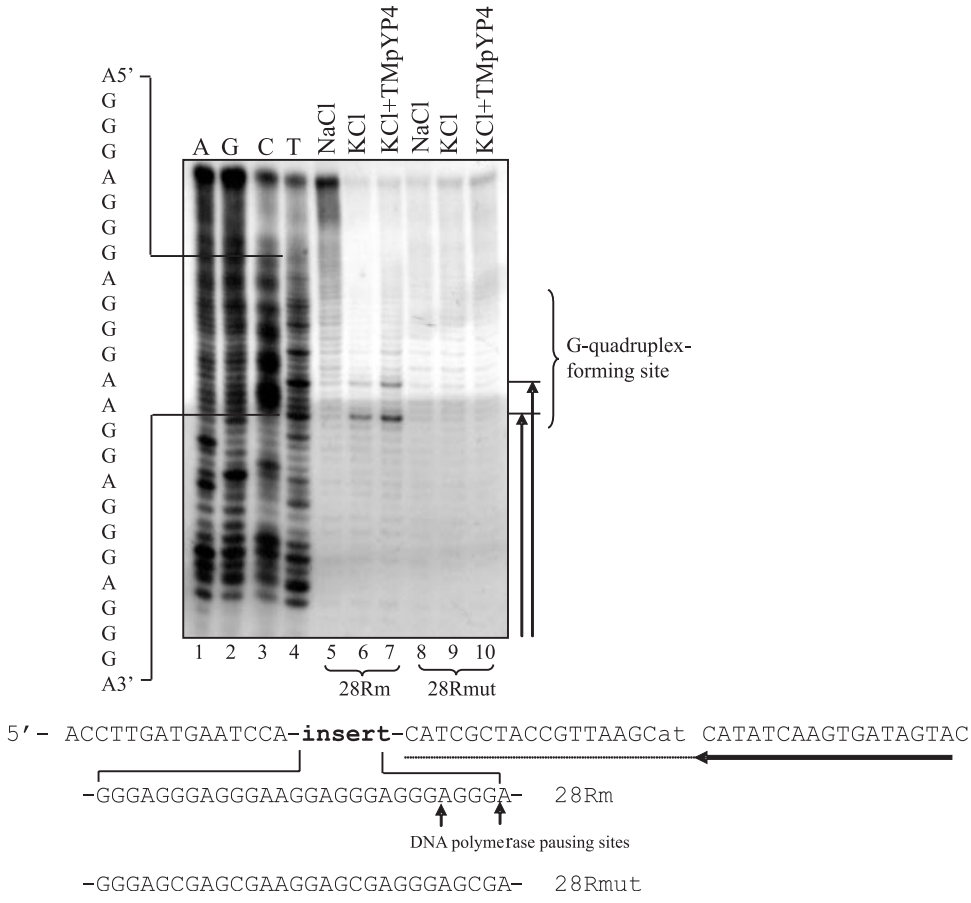


**Figure 3.** Polymerase stop assay showing primer elongation by the Klenow fragment. The single-stranded templates containing either 28Rm or 28Rmut are shown. These DNA substrates have been incubated overnight in buffers containing NaCl, KCl or KCl and TMPyP4. A primer elongation reaction was performed for 30 min at 37°C. Elongation products were separated in a 15% polyacrylamide, 8 M urea, denaturing gel. Sequencing reactions by the Sanger dideoxy method, using the same primer of the polymerase stop assay, were carried out. Klenow fragment elongation pauses in correspondence of the adenine preceding the first and second runs of guanines at the 3′ end of NHPPE, (positions are indicated by lines).

is potassium-dependent and stronger in the presence of TMPyP4. In this case too, a secondary and weaker pausing site is observed at the adenine preceding the second 3′ G-run. The polymerase stop assay was also performed with the human single- and double-stranded templates and obtained results similar to those observed for the parental mouse templates (data not shown).

### Determination of *KRAS* G-quadruplex structures by DMS footprinting

To determine the nature of the G-quadruplexes formed by the *KRAS* G-rich sequences, we probed the accessibility of guanine N7 to DMS. While in duplex and single-stranded DNA guanine N7 is available for methylation with DMS, in quadruplex DNA, being involved in a Hoogsteen hydrogen bond, N7 does not react with DMS. Figure 5 (left panel) shows the results of a methylation assay performed on the mouse 28Rm sequence in the denatured state (lanes 1–3), after incubation in KCl (lane 4) or KCl+TMPyP4 (lane 5). It can be seen that in the presence of KCl and TMPyP4, most guanines are protected from methylation and thus involved in G-tetrads, except G14 and G15 and, to a lesser extent G17–G19. Taking into account the CD, PAGE and primer extension experiments, we propose for this promoter sequence an intramolecular parallel G-quadruplex that consists of three G-tetrads, two one-base and one nine-base external loops (structure Q[1/1/9], left). Such a propeller type quadruplex conformation has been found for the telomere d[AGGG(TTAGGG)3] in the crystalline state (34). Since primer extension experiments showed a secondary polymerase pause at the adenine preceding the second 3′ G-run, an alternative quadruplex with two one-base and a 5-base external loops, called Q[1/1/5], can be formed. Of the two quadruplex loop isomers, Q[1/1/9] should have a higher stability, according to polymerase stop assays. As the topology of the loops cannot be predicted from DMS footprinting data, we cannot rule out that the 9-base loop of Q[1/1/9] has a diagonal topology as depicted in Q[1/1/9], right. Interestingly, when a guanine in the G-runs involved in the tetrads is substituted with cytosine, the resulting 4-base mutant sequence exhibits a dramatically different DMS-induced cleavage pattern, where all the guanines are modified and cleaved by DMS/piperidine. This suggests that 28Rmut does not adopt a quadruplex structure, in perfect accord with CD, PAGE and primer extension experiments.

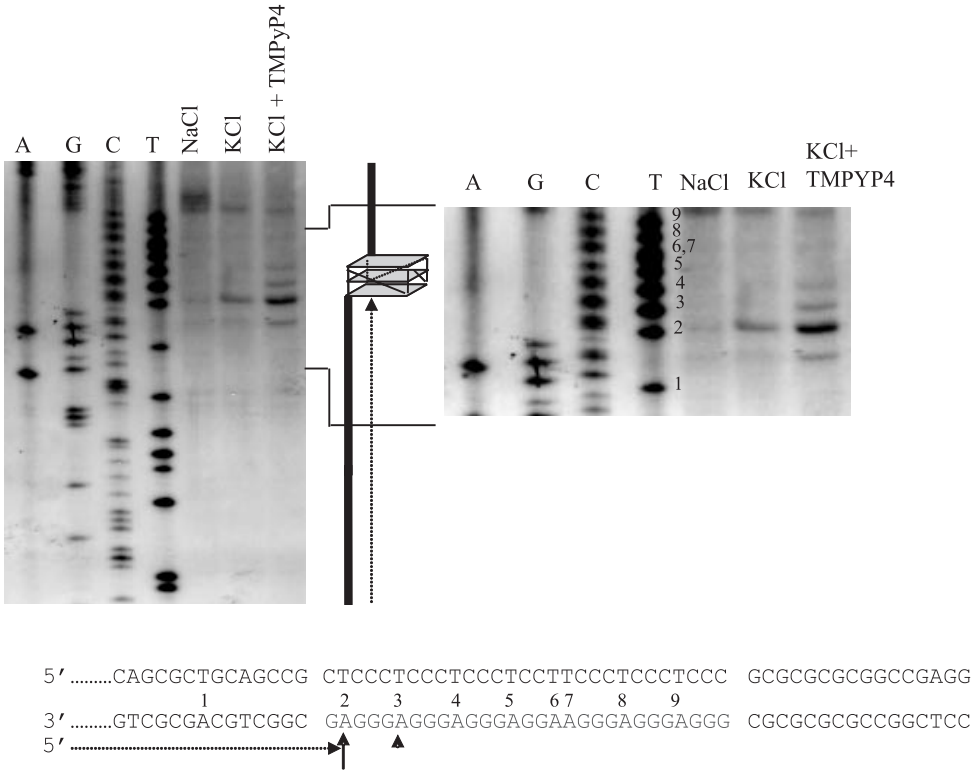


**Figure 4.** Polymerase stop assay performed with a double-stranded template (plasmid pKRS-413). In this experiment pKRS-413, containing the mouse *KRAS* promoter, has been incubated in 100 mM NaCl, 100 mM KCl or 100 mM KCl and 100 nM TMPyP4 at 45°C for 48 h. A primer elongation reaction was performed, using a primer located downstream from the G-rich strand. Reactions were performed as described in Figure 3. The adenines in the G-rich sequence are numbered.

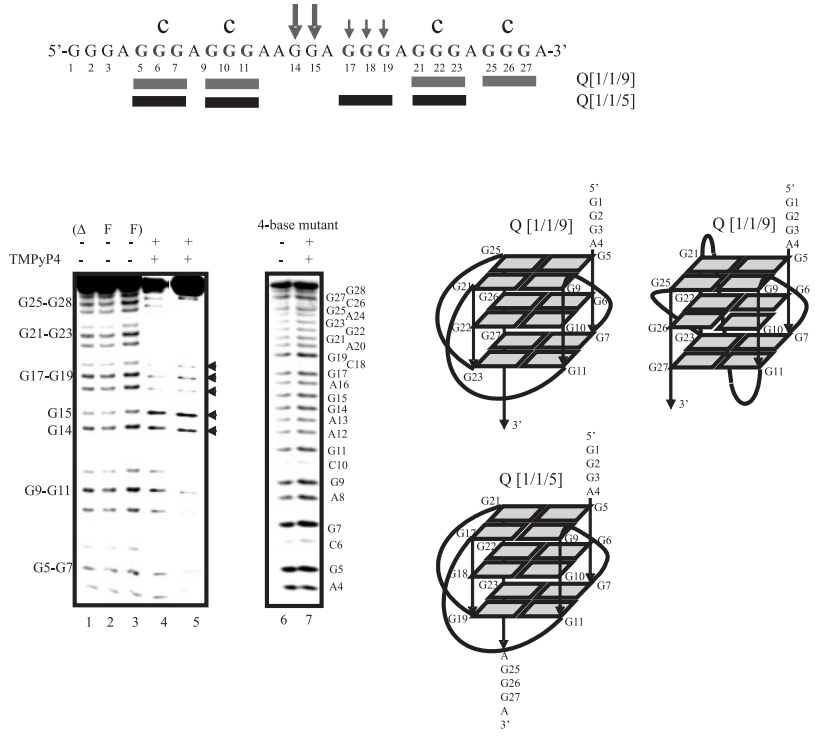


**Figure 5.** (Top) Sequence of the mouse G-rich motif 28Rm subjected to DMS footprinting. The four guanines that are substituted with cytosines in 28Rmut are indicated (Bottom) DMS footprintings of the G-rich strand of NHPPE (28Rm) and 4-base mutant 28Rmut. DMS-induced cleavage of denatured 28Rm (lanes 1–3, F = formamide, Δ = heating); 28Rm after incubation in 100 mM KCl (lane 4) or 100 mM KCl plus 100 nM TMPyP4 (lane 5); 28Rmut in F (lane 6) and 100 mM KCl plus 100nM TMPyP4 (lane 7). The guanines cleaved by the DMS/piperidine treatment are labelled in the right side of the sequencing gel. (Bottom right) G-quadruplex structures proposed for 28Rm, based on DMS footprinting, CD, electrophoretic mobility and polymerase stop assays.

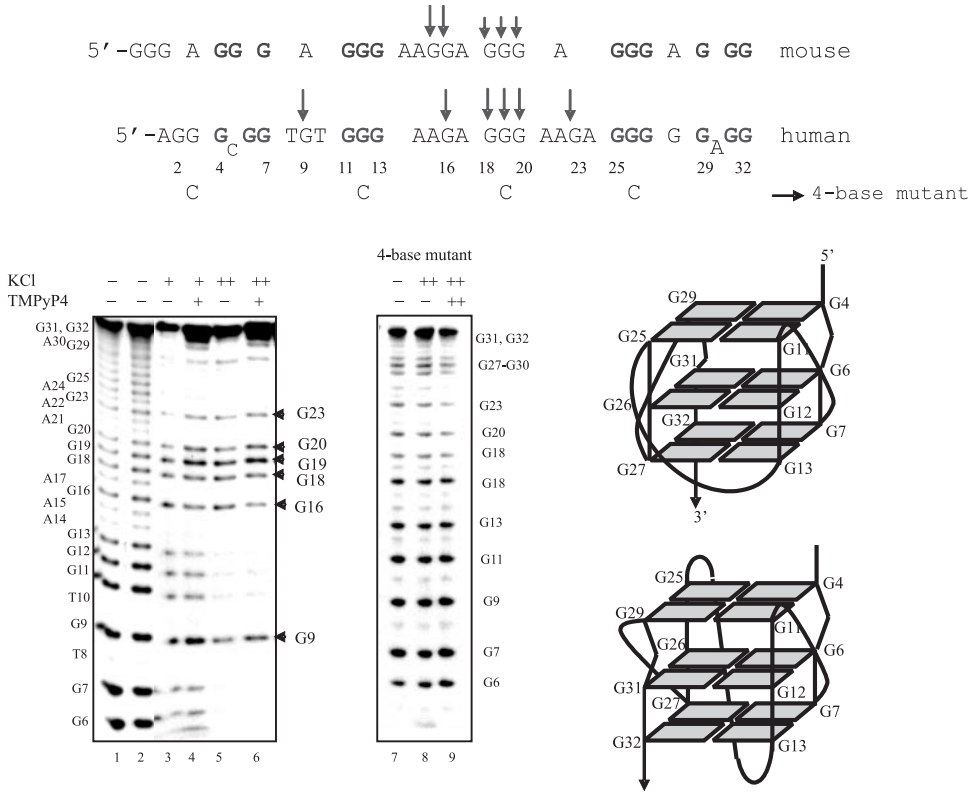


**Figure 6.** (Top) Sequence of the human G-rich motif 32Rh subjected to DMS footprinting. The guanines that are substituted with cytosines in 32Rmut are indicated. The parental 28Rm mouse sequence is also shown for comparison. Arrows indicate the cleavage sites (Bottom) DMS footprinting of the G-rich strand of the human NHPPE (32Rh) and of the corresponding 4-base mutant 32Rmut. DMS-induced cleavage of the denatured 32Rm (lanes 1-2); 32Rh after incubation in 50 mM KCl (lane 3) or 50 mM KCl plus 50 nM TMPyP4 (lane 4); 32Rh in 100 mM KCl (lane 5) or 100 mM KCl plus 100 nM TMPyP4 (lane 6); 32Rmut in formamide (lane 7), in 100 mM KCl (lane 8), in 100 mM KCl plus 100 nM TMPyP4 (lane 9). The guanines cleaved by the DMS/piperidine treatment are labelled in the right side of the sequencing gel.

Figure 6 shows the DMS footprinting for the human G-rich sequence. In this sequence the guanines are distributed less regularly than in the mouse sequence and three pyrimidines disrupt the polypurine motif. However, when the two sequences are aligned one against the other, their sequence homology appears evident. In the presence of KCl (lanes 3 and 5) or KCl+TMPyP4 (lanes 4 and 6), a precise cleavage pattern is obtained, with G9, G16, G18, G19, G20 and G23 showing a high reactivity with DMS. This cleavage profile shares common features with the profile obtained with the mouse sequence and supports the formation of a parallel G-quadruplex stabilized by three G-tetrads and three external loops (or two external and one diagonal loops), as the G-quadruplex proposed for the mouse sequence. Note that G29, but not the expected G28, is methylated by DMS: this is probably due to the fact that TMPyP4 interacts with the adenine bridging G29 and G31 rather than with G28 in the miniloop. Again, the 4-base mutant sequence did not show any footprint. To futher support the quadruplex structure proposed for the human *KRAS* sequence we compared the $T_m$ and CD spectrum of 32Rh with those relative to a number of mutant sequences. Interestingly, we did not observe changes in CD shape and $T_m$ when G18, G19, G20 or G9, G16, G23, were replaced with thymidines. Conversely, when guanines involved in a G-tetrad such as G12, G26 or G29 were substituted with thymidines, dramatic changes in both the CD and $T_m$ were observed (data not shown).

### Interaction between TMPyP4 with *KRAS* quadruplexes

Previous studies have demonstrated that the cationic porphyrin TMPyP4 stabilizes quadruplex DNA (37–40). We first examined the interaction between TMPyP4 and the mouse *KRAS* G-quadruplex by CD experiments. Figure 7A shows the CD spectra of 3 μM 28Rm incubated in KCl or KCl with three equivalents of TMPyP4. Although TMPyP4 is achiral, a negative ellipticity appeared in the region of the porphyrin Soret band (∼430 nm) as a result of the binding of the ligand to the G-quadruplex. To determine the stabilizing effect of TMPyP4 on the mouse quadruplex, we measured the CD spectrum as a function of temperature, finding that the $T_m$ increased from 75 to >95°C (at 95°C the quadruplex was not yet denatured). To gain insight into the interaction between the cationic porphyrin and the mouse *KRAS* G-quadruplex, we performed photocleavage experiments. TMPyP4 catalyses the oxidation of DNA upon exposure to light, resulting in DNA strand breakage in proximity of the binding sites (38). The photocleavage of 28Rm and its correspondent 4-base mutant sequence 28Rmut is shown in

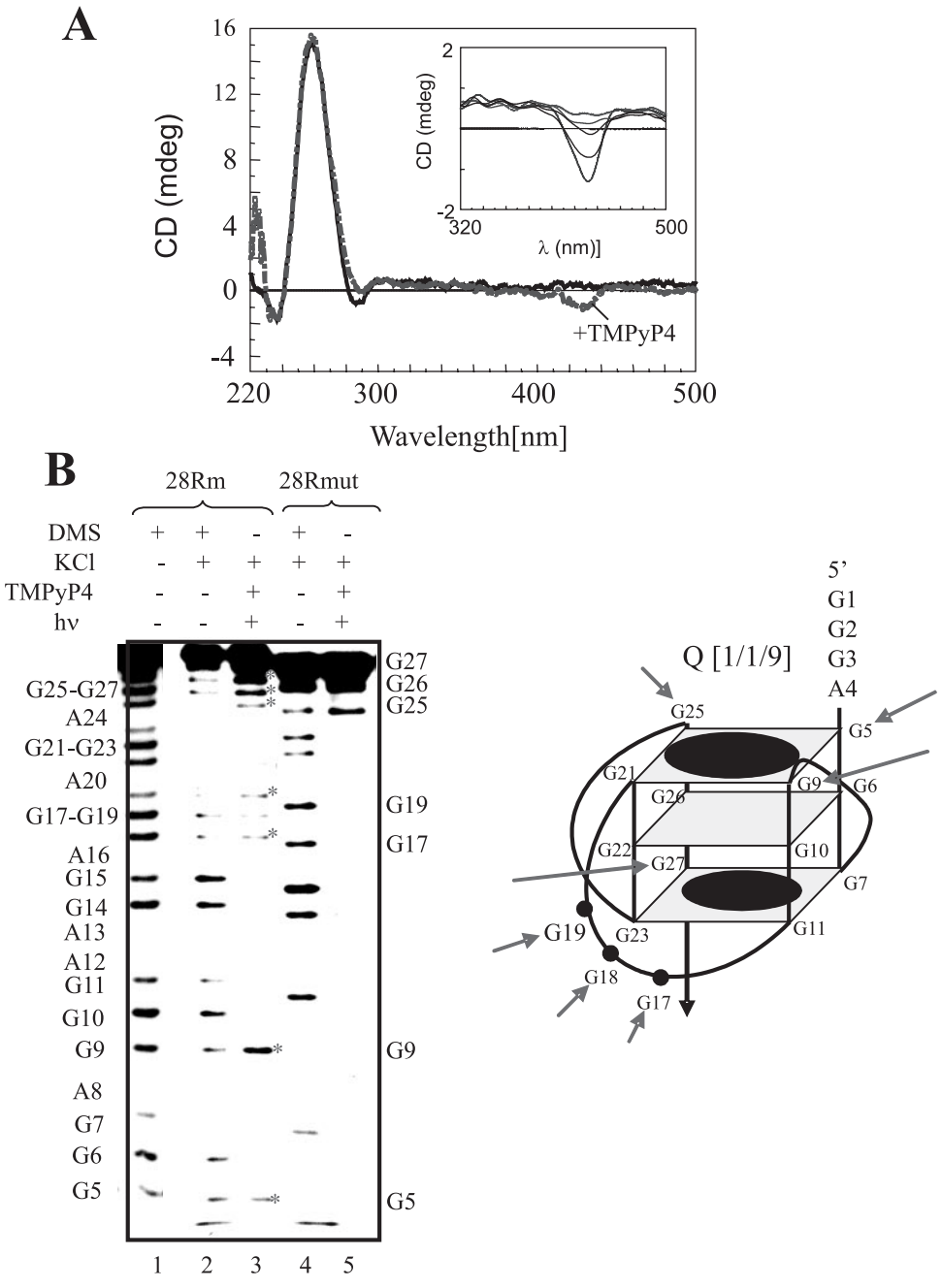


**Figure 7.** (**A**) CD spectra of the mouse G-rich sequence 28Rm in the presence of 100 mM KCl with and without TMPyP4. The ellipticity arising from the 28Rm-porphyrin interaction is shown in the inset. DNA concentration is 3 μM, TMPyP4 increased from 3 to 18 μM. Cuvette pathlength 0.5 cm. (**B**) Photocleavage of the G-quadruplex formed by the mouse 28Rm sequence. DMS-induced cleavage of 28Rm in the denatured state (lane 1), under a quadruplex conformation (lane 2); photocleavage of 28Rm in the quadruplex conformation (lane 3); DMS-induced cleavage of 28Rmut (lane 4), Photocleavage of 28Rmut (lane 5). Right structure shows with arrows the guanines that are photocleaved.

Figure 7B. The two oligonucleotides show a distinct photocleavage pattern. Considering that TMPyP4 stabilizes the quadruplex isomer with a 9-base loop, the DNA photodamage occurs to the guanines of the external G-tetrads (G5, G9, G25 and G27, indicated with red arrows) and the guanines in the nine-base loop (G17, G18, G19, blue arrows). As G26, although located in the internal G-tetrad, is cleaved may be due to the fact that a fraction of 28Rm adopts the Q[1/1/5] conformation, in which the first 3′ run of guanines is excluded to the structure and is free to interact electrostatically with TMPyP4. In conclusion, the data support the notion that TMPyP4 binds to the mouse *KRAS* quadruplex by end-stacking to the external G-tetrads and electrostatically to the bases of the larger loop. These modes of binding are in keeping with previous results obtained with telomeric DNA (39) and with the *CMYC* quadruplex (17).

### Quadruplex-stabilizing TMPyP4 strongly inhibits the activity of the of *KRAS* promoter

The critical role played on transcription by the *KRAS* NHPPE sequence motif has been demonstrated elsewhere (13,14). Considering that NHPPE extrudes a G-quadruplex structure, that is strongly stabilized by TMPyP4, we wished to evaluate if this unusual DNA conformation does affect transcription. It has been shown that TMPyP4 inhibits telomerase (41), helicase-mediated unwinding of G-quadruplex structures (42) and downregulates the expression of *CMYC,* whose promoter also forms a G-quadruplex (43). In order to investigate the effect of the cationic porphyrin on the activity of the *KRAS* promoter, we co-transfected 293 cells with plasmid pKRS-413, bearing the mouse *KRAS* promoter upstream from the reporter CAT gene, plasmid pTK β-gal as a control and increasing quantities of TMPyP4 (up to 20 μM). We measured the expression of CAT relatively to that of β-gal by ELISA assays, 48 h after transfection (Figure 8). We found that at all the concentrations used, TMPyP4 reduced the expression of CAT to 20% of the control, indicating that the stabilization of the G-quadruplex has a strong repression effect on transcription. This experiment suggests that the quadruplex structure formed locally in the mouse *KRAS* promoter at NHPPE behaves as a transcription repressor.

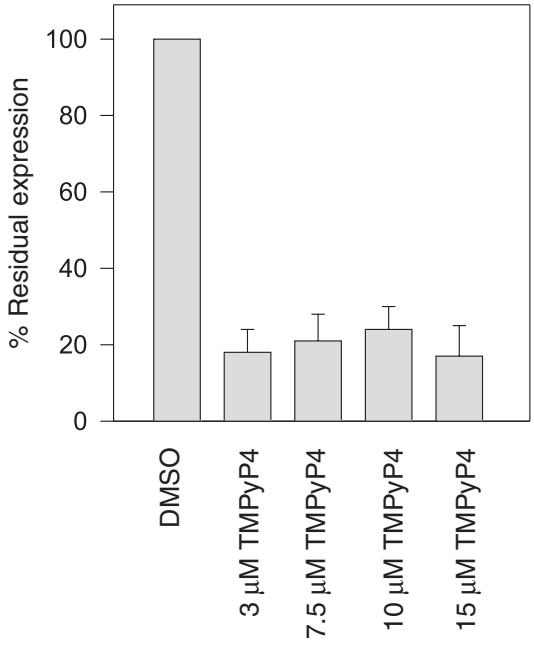


**Figure 8.** Chloramphenicol acetyl transferase expression assay to determine the effect of TMPyP4 on the activity of *KRAS* promoter. Plasmid pKRS-413, containing CAT driven by the mouse *KRAS* promoter, has been transfected in 293 cells in the presence of increasing amounts of TMPyP4. As a control for transfection efficiency and aspecific transcription impairment plasmid pTK-βgal was cotrasfected with pKRS-413. The expression of CAT, with respect to that of β-gal, was determined by an ELISA assay, 48 h after transfection. The residual CAT expression, (CAT/β-gal) × 100, is reported in the histograms. The values are the average of three independent experiments in duplicate. Error bar are ±SE. These experiments showed that stabilization of G-quadruplex formed within NHPPE following cell treatment with TMPyP4, decreased the expression of a reporter gene driven by the KRAS promoter.

### *KRAS* G-quadruplex recognises nuclear proteins

The NHPPE of *KRAS* is the target of nuclear proteins (14). Little is known about these proteins except that they bind to a promoter region that plays an essential role for transcription. We performed EMSA with NIH 3T3 nuclear extracts and the mouse $^{32}$P-labelled NHPPE duplex as a probe. Figure 9A shows that three protein–DNA complexes (M1–M3) are formed. These binding activities are sequence-specific, as the experiments have been carried out in the presence of a large excess of polyd(I–C). When increasing amounts of cold G-rich oligonucleotide 28Rm and 32Rh, mimicking the mouse and human *KRAS* G-quadruplexes, are added to the reaction mixture, they effectively competed with the probe for protein binding. An oligonucleotide concentration 100-fold in excess over probe (radiolabelled NHPPE duplex, 5 nM), is sufficient to abrogate the interaction responsible for the formation of complexes M1 and M2 (lanes 4 and 7), whereas the 4-base mutant oligonucleotide 28Rmut, at identical concentrations, had no effect (lanes 8–10). This indicates that the proteins in M1 and M2 are recognized not only by the NHPPE duplex but also by the G-quadruplexes formed by the G-rich strands of mouse and human NHPPEs. The interaction between these proteins and the *KRAS* quadruplexes is highly stereospecific, as UGGGGU, forming a parallel quadruplex without loops (called Q1) (44), does not compete with the duplex probe (lane 14). EMSA experiments were also performed with nuclear extracts from human Panc-1 cells (Figure 9B). In this case we observed two DNA–protein complexes (H1 and H2) of which H1 is competed by the *KRAS* quadruplexes. Here too, no competition is observed with the 4-base mutant 28Rmut (lanes 6–8), Q1 and Q2, a G-quadruplex with lateral loops formed by GUUUUUGGGGCUUUUC (45) (lanes 11 and 12). Interestingly, the quadruplex formed by the G-rich sequence present in the *CMYC* promoter shows some competition with the duplex probe (lanes 13 and 14). When we used the human NHPPE duplex as probe, we practically obtained the same results (data not shown). To further characterize the binding between the mouse *KRAS* quadruplex and the nuclear proteins, we performed a Southwestern analysis (Figure 9C). Nuclear extracts from mouse NIH 3T3 (M) and human Panc-1 (H) cells were run in SDS–PAGE and assayed with $^{32}$P-labelled 28Rm in the quadruplex conformation and $^{32}$P-labelled 28Rmut. Three binding activities are observed with the mouse extract (at ∼32, 75 and 120 kDa), whereas only two bands (32 and 75 kDa) are obtained with the human extract. In accord with EMSA competition assays, the 4-base mutant oligonucleotides did not show any binding activity. To find out if the bands observed in the Southwestern blot are the subunits of a larger protein, we performed UV-cross linking experiments under native conditions, but unfortunately were not able to obtain reproducible results. Finally, we addressed the question if the proteins that bind to both the quadruplex and duplex conformations of mouse NHPPE are essential for *KRAS* transcription. We reasoned that an oligonucleotide mimicking the mouse *KRAS* G-quadruplex should behave as an aptamer and cause a transcription repression if the proteins that it binds to are essential for transcription. As proof of principle we transfected 293 cells with plasmid pKRS-413, containing CAT driven

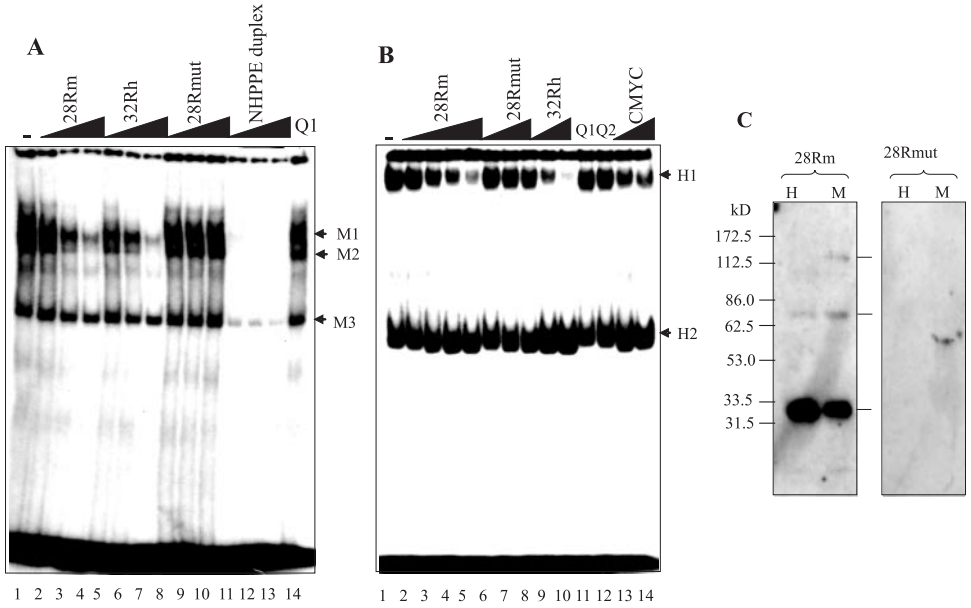


**Figure 9.** DNA–protein competition experiments. (**A**) EMSA showing that $^{32}$P-labelled mouse NHPPE duplex (5 nM) binds to three nuclear proteins from a mouse NIH 3T3 cell extract (M1–M3) (lane 1). The competitors are: quadruplex 28Rm (lanes 2–4, 10-/50-/100-fold over the labelled duplex probe); quadruplex 32Rh (lanes 5–7, 10-/50-/100-fold), 4-base mutant 28Rmut (lanes 8–10, 10-/50-/100-fold), target duplex (10-/50-/100-fold) (lanes 11–13); quadruplex Q1 (for sequences see Table 1) (lane 14, 100-fold excess over probe) (lane 14). The autoradiography was analysed with a Gel Doc 2000 Imager System (Bio-Rad) and the percent OD in bands M1 and M2 respect to total OD in the lane was calculated. Set to 100 the value obtained in lane 1 (control), the values of M1+M2 in lanes 1–14 are 100, 92, 63, 29, 73, 46, 24, 88, 81, 99, 1, 0, 0 and 82, respectively. These values provide a quantitative estimate of the competition capacity of the tested oligonucleotides; (**B**) EMSA showing the $^{32}$P-labelled mouse NHPPE duplex (5 nM) binds to two nuclear proteins from human Panc-1 cells (H1 and H2) (lane 1). The competitors are quadruplex 28Rm (lanes 2–5, 10-/20-/50-/100-fold over the probe); quadruplex 32Rh (lanes 9–10, 50-/100-fold); 4-base mutants 28Rmut (lanes 6–8, 10-/50-/100-fold); quadruplexes Q1 and Q2 (for sequences see Table 1) (lanes 11 and 12, 100-fold excess over probe); quadruplex *CMYC* (sequence in Table 1) (lanes 13, 14, 50-/100-fold); Percent OD in H1 respect to total OD, measured in the lanes 1–14 are 100, 94, 77, 60, 41, 79, 77, 77, 46, 27, 83, 87, 68 and 69; (**C**) Southwestern blots showing that 28Rm, but not the 4-base mutant 28Rmut, binds to nuclear proteins of 32, 75 and 115 kDa. The letters H and M on the top panels indicate human and mouse nuclear extracts, respectively. The mobilities of marker proteins are shown on the left.

by the mouse *KRAS* promoter, pTK β-gal and 1 μM oligonucleotides 28Rm, 32Rh, 28Rmut and 32Rmut. The results obtained are reported in Figure 10A which shows that the *KRAS* transcription is reduced up to 40% of the control in the presence of the quadruplex-forming oligonucleotides. This is observed with both mouse and human G-quadruplexes, indicating that the protein(s) binding to the *KRAS* G-quadruplex is(are) essential elements for transcription.

## DISCUSSION

In this work we have demonstrated that the G-rich strand of NHPPE, located within the proximal promoter region of *KRAS*, is able to form a G-quadruplex structure that seems to be involved in the mechanism of transcription regulation. As the NHPPEs present in the human and mouse *KRAS* genes share a high sequence homology (Figure 1), this structural polymorphism is observed in both gene promoters. In order to gain insight into the nature of these quadruplexes, we performed spectroscopic and enzymatic experiments. CD (strong ellipticity at 260 nm) and UV TDS (maximum at 273 nm) showed spectral features indicative of the formation of a parallel G-quadruplex structure (27,46). To discover whether the *KRAS* quadruplexes are intra- or intermolecular, we analysed the mobility of the G-rich sequences in a native polyacrylamide gel. As they migrated much faster than the corresponding NHPPE duplexes and slightly slower than the 4-base mutants, we concluded that they assume an intramolecular folded quadruplex. The *KRAS* G-quadruplexes were sufficiently stable [$T_m$ = 64°C (human) and 73°C (mouse) in 100 mM KCl] to act as a barrier for DNA polymerase. The arrest of DNA synthesis was found to be $K^+$-dependent and stronger in the presence of the cationic porphyrin TMPyP4, which is known to stabilize quadruplex DNA (38,39). The polymerase stop assays were performed with both single- and double-stranded templates and showed that the main arrest of DNA polymerase occurred at the base preceding the first run of guanines at the 3′ side of the G-rich sequence. However, a secondary enzymatic pause was observed at the beginning of the second G-run, in keeping with the formation of two quadruplex structures within the mouse G-rich strand. An in-depth investigation on the structure of the *KRAS* G-quadruplexes was obtained by DMS-footprinting experiments. The cleavage patterns obtained with the two *KRAS* G-rich sequences are consistent with the formation of a parallel G-quadruplex structure characterized by three G-tetrads and three loops. As DMS-footprinting data do not give information about the topology of the loops, the three loops may be either all external (propeller conformation), as found in the telomere d[AGGG(TTAGGG)3] repeat in the crystalline state (34), or two external and one diagonal, as depicted in the structures of Figures 5 and 6. Moreover, as the mouse G-rich sequence comprises six runs of guanines, two quadruplexes are formed, as suggested

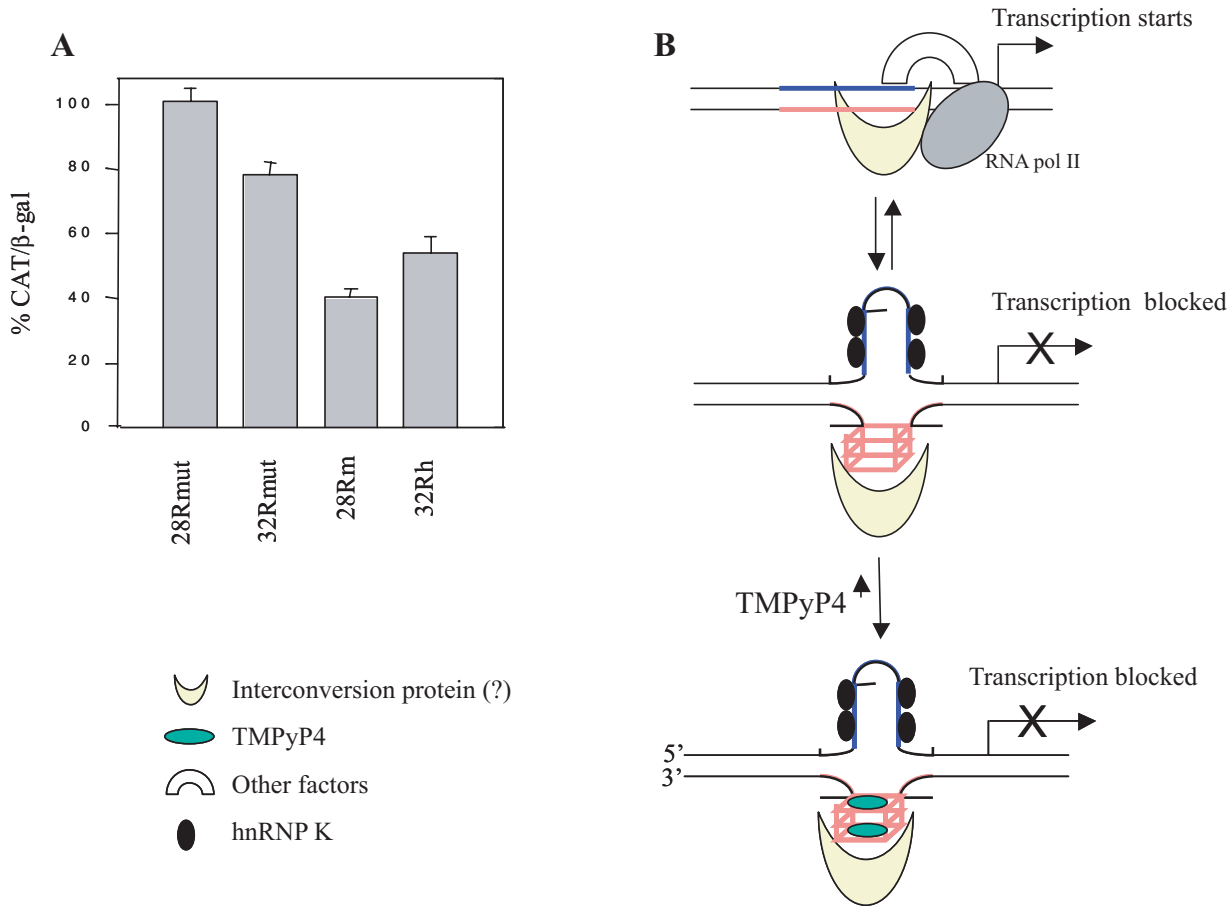


**Figure 10.** (**A**) CAT assay to determine the effect of 28Rm and 32Rh on *KRAS* transcription. Cells 293 were co-transfected with plasmid pKRS-413, pTK-βgal and 1 μM quadruplex-forming oligonucleotide (28Rm, 32Rh) or 4-base mutant (28Rmut, 32Rmut). The expression of CAT with respect to that of β-gal, was determined by an ELISA assay, 48 h after transfection. The residual CAT expression, (CAT/β-gal) × 100, is reported in the histograms. The values are the average of three independent experiments in duplicate. Error bars are ±SE. (**B**) Model for regulation of transcription in the *KRAS* gene.

by the double arrest observed in the DNA polymerase stop assay. In nice accord with CD and polymerase stop assays, the 4-base mutants did not give a DMS footprinting. The cationic porphyrin TMPyP4 was found to stabilize the G-quadruplexes by ∼20°C. According to photocleavage experiments, the porphyrin should stack to the external G-tetrads of the mouse quadruplex and also interacts electrostatically with the bases of the larger loop. To uncover the biological function of the *KRAS* G-quadruplex, we transfected 293 cells with increasing amounts of TMPyP4 and vector pKRS-413, containing CAT driven by the mouse *KRAS* promoter. We found that the porphyrin promoted a strong suppression of CAT to ∼20% of control, suggesting that the G-quadruplex acts as a transcription repressor. A similar result has been observed for *CMYC*, whose promoter also contains a polypurine–polypyrimidine motif forming a G-quadruplex (17,18). Although in these transfection experiments TMPyP4 has not been site-directed against genomic *KRAS*, the formation of a G-quadruplex in a critical region of *KRAS* raises the intriguing possibility that this unorthodox structure is somehow involved in transcription regulation. This hypothesis is supported by the results obtained with EMSA experiments. The mouse NHPPE duplex shows three binding activities when incubated with nuclear extracts obtained from mouse NIH 3T3 cells, namely M1, M2 and M3. The single-stranded G-rich sequences of the mouse and human *KRAS* genes competed with the duplex probe for the binding to proteins in M1 and M2, but not in M3. The competition is observed with the quadruplex-forming wild-type sequences but not with the 4-base mutant sequences. Interestingly, when the interaction between the mouse NHPPE duplex and nuclear proteins was competed by oligonucleotides forming G-quadruplexes with conformations different from that proposed for *KRAS* (i.e. quadruplexes without loops or with two lateral loops) no competition activity was observed. The parallel quadruplex formed by the G-rich sequence present in the *CMYC* promoter (47) was able to compete partially with the duplex probe. These findings suggest that the interaction between proteins M1/M2 and the G-rich strand of *KRAS* is stereospecific and mediated by the particular quadruplex structure assumed by this sequence motif. In a previous study Michelotti *et al.* (48) have reported a zinc-dependent binding activity by the guanine-rich element of the *CMYC* promoter. This purine-rich strand binding protein was identified as being CNBP: a cellular nucleic acid binding protein implicated in the regulation of sterol responsive genes. One could wonder if one of proteins (M1 or M2; H1) that recognize the *KRAS* quadruplex is

protein CNBP. This is not the case, as CNBP in a SDS–polyacrylamide gel migrates with only one band of 20 kDa, whereas the *KRAS* quadruplexes show in the SDS-polyacrylamide gel two binding activities: one at 32 kDa, the other at 75 kDa. Moreover, we observed that the interaction between H1 and the *KRAS* quadruplex is not abrogated by EDTA, i.e. it is not $Zn^{2+}$-dependent in the same way as is the interaction between the *CMYC* sequence and CNBP (data not shown).

Proteins binding sequence-specifically both the double-stranded and single-stranded polypyrimidine motifs have been reported as being hnRNP K (49,50) and NDPK-B (51). The former recognizes a distinct sequence segment, namely CTTCC, which is present in the human (two copies) and mouse (one copy) *KRAS* NHPPEs. How can these nuclear factors binding to the *KRAS* NHPPE duplex be correlated with the G-quadruplex conformation adopted by NHPPE? In Figure 10B we propose a scheme according to which *KRAS* NHPPE should exist in equilibrium between double-stranded and G-quadruplex conformations. When this structural equilibrium shifts towards the quadruplex conformation, the transcription should be repressed. This is suggested by the transfection experiments with TMPyP4 and by the results obtained with the *CMYC* promoter (17). Thus, it is possible that the quadruplex conformation behaves as negative regulator for *KRAS*. The unpaired polypyrimidine strand should interact with the single-stranded binding protein hnRNP K (49,50). To activate transcription, NHPPE should assume its canonical double-stranded conformation, but this is possible if the polypurine strand loses its unusual structure. As the duplex-to-quadruplex transformation is probably a slow process, it could be facilitated by a protein. It is likely that one of the proteins recognising both the duplex and quadruplex forms of NHPPE is involved in the duplex-to-quadruplex interconversion. This provides a rational for the finding that 293 cells transfected with a G-rich oligonucleotide mimicking the *KRAS* quadruplex reduces the activity of the *KRAS* promoter to 40% of the control (4-base mutant sequence). In the light of these results, oligonucleotides mimicking the *KRAS* quadruplexes may have a potential anticancer activity, as they interfere with the expression of *KRAS*. This is supported by the data presented in this paper and by previous data obtained with a stable transfectant cell line generating constitutively a quadruplex-forming oligoribonucleotide that strongly impairs cell proliferation (11). Another attractive target for small ligands is the *KRAS* NHPPE quadruplex. The selection from a chemical library of molecules that specifically bind to the *KRAS* G-quadruplex could be an interesting approach for the development of powerful anticancer drugs against refractory pancreatic adenocarcinomas cells.

## SUPPLEMENTARY DATA

Supplementary Data are available at NAR Online.

## ACKNOWLEDGEMENTS

This work has been carried out with the financial support of Ministry of Education (PRIN 2005). Funding to pay the Open Access publication charges for this article was provided by MIUR.

*Conflict of interest statement*. None declared.

## REFERENCES

1. Li,D., Xie,K., Wolff,R. and Abbruzzese,J.L. (2004) Pancreatic cancer. *Lancet*, **363**, 1049–1057.
2. Sohn,T.A. and Yeo,C.J. (2000) The molecular genetics of pancreatic ductal carcinoma: a review. *Surg. Oncol.*, **9**, 95–101.
3. Chin,L., Tam,A., Pomerantz,J., Wong,M., Holash,J., Bardeesy,N., Shen,Q., O'Hagan,R., Pantginis,J., Zhou,H. *et al.* (1999) Essential role for oncogenic Ras in tumour maintenance. *Nature*, **400**, 468–472.
4. Adjei,A.A. (2001) Blocking oncogenic Ras signaling for cancer therapy. *J. Natl Cancer Inst.*, **93**, 1062–1074.
5. Smit,V.T., Boot,A.J., Smits,A.M., Fleuren,G.J., Cornelisse,C.J. and Bos,J.L. (1988) KRAS codon 12 mutations occur very frequently in pancreatic adenocarcinomas. *Nucleic Acids Res.*, **16**, 7773–7782.
6. Hingorani,S.R., Petricoin,E.F., Maitra,A., Rajapakse,V., King,C., Jacobetz,M.A., Ross,S., Conrads,T.P., Veenstra,T.D., Hitt,B.A. *et al.* (2003) Preinvasive and invasive ductal pancreatic cancer and its early detection in the mouse. *Cancer Cell*, **4**, 437–450.
7. Kita,K., Saito,S., Morioka,C.Y. and Watanabe,A. (1999) Growth inhibition of human pancreatic cancer cell lines by anti-sense oligonucleotides specific to mutated K-ras genes. *Int. J. Cancer*, **80**, 553–558.
8. Giannini,C.D., Roth,W.K., Piiper,A. and Zeuzem,S. (1999) Enzymatic and antisense effects of a specific anti-Ki-ras ribozyme *in vitro* and in cell culture. *Nucleic Acids Res.*, **27**, 2737–2744.
9. Cogoi,S., Rapozzi,V., Quadrifoglio,F. and Xodo,L. (2001) Anti-gene effect in live cells of AG motif triplex-forming oligonucleotides containing an increasing number of phosphorothioate linkages. *Biochemistry*, **40**, 1135–1143.
10. Cogoi,S., Ballico,M., Bonora,G.M. and Xodo,L.E. (2004) Antiproliferative activity of a triplex-forming oligonucleotide recognizing a Ki-ras polypurine/polypyrimidine motif correlates with protein binding. *Cancer Gene Ther.*, **11**, 465–476.
11. Cogoi,S., Quadrifoglio,F. and Xodo,L.E. (2004) G-rich oligonucleotide inhibits the binding of a nuclear protein to the Ki-ras promoter and strongly reduces cell growth in human carcinoma pancreatic cells. *Biochemistry*, **43**, 2512–2523.
12. Sebti,S.M. and Hamilton,A.D. (2000) Farnesyltransferase and geranylgeranyl-transferase I inhibitors and cancer therapy: lessons from mechanism and bench-to-bedside translational studies. *Oncogene*, **19**, 6584–6593.
13. Jordano,J. and Perucho,M. (1986) Chromatin structure of the promoter region of the human c-K-ras gene. *Nucleic Acids Res.*, **14**, 7361–7378.
14. Hoffman,E.K., Trusko,S.P., Murphy,M. and George,D.L. (1990) An S1 nuclease-sensitive homopurine/homopyrimidine domain in the c-Ki-ras promoter interacts with a nuclear factor. *Proc. Natl Acad. Sci USA*, **87**, 2705–2709.
15. Behe,M.J. (1995) An overabundance of long oligopurine tracts occurs in the genome of simple and complex eukaryotes. *Nucleic Acids Res*, **23**, 689–695.
16. Postel,E.H., Mango,S.E. and Flint,S.J. (1989) A nuclease-hypersensitive element of the human c-myc promoter interacts with a transcription initiation factor. *Mol. Cell Biol.*, **9**, 5123–5133.
17. Siddiqui-Jain,A., Grand,C.L., Bearss,D.J. and Hurley,L.H. (2002) Direct evidence for a G-quadruplex in a promoter region and its targeting with a small molecule to repress c-MYC transcription. *Proc. Natl Acad. Sci USA*, **99**, 11593–11598.
18. Simonsson,T., Pecinka,P. and Kubista,M. (1998) DNA tetraplex formation in the control region of c-myc. *Nucleic Acids Res.*, **26**, 1167–1172.
19. Gilmour,D.S., Thomas,G.H. and Elgin,S.C. (1989) *Drosophila* nuclear proteins bind to regions of alternating C and T residues in gene promoters. *Science*, **245**, 1487–1490.
20. Sun,D., Guo,K., Rusche,J.J. and Hurley,L.H. (2005) Facilitation of a structural transition in the polypurine/polypyrimidine tract within the proximal promoter region of the human VEGF gene by the presence of potassium and G-quadruplex-interactive agents. *Nucleic Acids Res.*, **33**, 6070–6080.

21. Mavrothalassitis,G.J., Watson,D.K. and Papas,T.S. (1990) Molecular and functional characterization of the promoter of ETS2, the human c-ets-2 gene. *Proc. Natl Acad. Sci USA*, **87**, 1047–1051.
22. Vigneswaran,N., Thayaparan,J., Knops,J., Trent,J., Potaman,V., Miller,D.M. and Zacharias,W. (2001) Intra- and intermolecular triplex DNA formation in the murine c-myb proto-oncogene promoter are inhibited by mithramycin. *Biol. Chem.*, **382**, 329–342.
23. Roebroek,A.J., Schalken,J.A., Verbeekm,J.S., Van den Ouweland,A.M., Onnekink,C., Bloemers,H.P. and Van de Ven,W.J. (1985) The structure of the human c-fes/fps proto-oncogene. *EMBO J.*, **4**, 2897–2903.
24. Bonham,K. and Fujita,D.J. (1993) Organization and analysis of the promoter region and 5′ non-coding exons of the human c-src proto-oncogene. *Oncogene*, **8**, 1973–1981.
25. Dignam,J.D. (1990) Preparation of extracts from higher eukaryotes. *Methods Enzymol.* **182**, 194–203.
26. Sen,D. and Gilbert,W.A. (1990) Sodium-potassium switch in the formation of four-stranded G4-DNA. *Nature (London)*, **344**, 410–414.
27. Rujan,I.N., Meleney,J.C. and Bolton,P.H. (2005) Vetebrate telomere repeat DNAs favour external loop propeller quadrupelx structures in the presence of high concentrations of potassium. *Nucleic Acids Res.*, **33**, 2022–2031.
28. Aboul-ela,F., Murchie,A.I. and Lilley,D.M. (1992) NMR study of parallel-stranded tetraplex formation by the hexadeoxynucleotide d(TG4T). *Nature*, **360**, 280–282.
29. Matsugami,A., Okuizumi,T., Uesugi,S. and Katahira,M. (2003) Intramolecular higher order packing of parallel quadruplexes comprising a G:G:G:G tetrad and a G(:A):G(:A):G(:A):G heptad of GGA triplet repeat DNA. *J. Biol. Chem.*, **278**, 28147–28153.
30. Mergny,J.-L., Phan,A.-T. and Lacroix,L. (1998) Following G-quartet formation by UV-spectroscopy. *FEBS Lett.*, **435**, 74–78.
31. Mergny,J.-L., Li,J., Lacroix,L., Amrane,S. and Chaires,J.B. (2005) Thermal difference spectra: a specific signature for nucleic acid structures. *Nucleic Acids Res.*, **33**, e138.
32. Ambrus,A., Chen,D., Dai,J., Jones,R.A. and Yang,D. (2005) Solution structure of the biologically relevant G-quadruplex element in the human c-MYC promoter. Implications for G-quadruplex stabilization. *Biochemistry*, **44**, 2048–2058.
33. Seenisamy,J., Rezler,E.M., Powell,T.J., Tye,D., Gokhale,V., Joshi,C.S., Siddiqui-Jain,A. and Hurley,LH (2004) The dynamic character of the G-quadruplex element in the c-MYC promoter and modification by TMPyP4. *J. Am. Chem. Soc.*, **126**, 8702–8709.
34. Parkinson,G.N., Lee,M.P. and Neidle,S. (2002) Crystal structure of parallel quadruplexes from human telomeric DNA. *Nature*, **417**, 876–880.
35. Vorlickova,M., Chladkova,J., Kejnovska,I., Fialova,M. and Kypr,J. (2005) Guanine tetraplex topology of human telomere DNA is governed by the number of (TTAGGG) repeats. *Nucleic Acids Res.*, **33**, 5851–5860.
36. Weitzmann,M.N., Woodford,K.J. and Usdin,K. (1996) The development and use of a DNA polymerase arrest assay for the evaluation of parameters affecting intrastrand tetraplex formation. *J. Biol. Chem.*, **271**, 20958–20964.
37. Han,H., Hurley,L.H. and Salazar,M. (1999) A DNA polymerase stop assay for G-quadruplex-interactive compounds. *Nucleic Acids Res.*, **27**, 537–542.
38. Wheelhouse,R.T., Sun,D., Han,H., Han,F.X. and Hurley,L.H. (1998) Cationic porphyrins as telomerase inhibitors: the interaction of tetra-(*N*-methyl-4-pyridyl)porphine with quadruplex DNA. *J. Am. Chem. Soc.*, **120**, 3261–3262.
39. Yamashita,T., Uno,T. and Ishikawa,Y. (2005) Stabilization of guanine quadruplex DNA by the binding of porphyrins with cationic side arms. *Bioorg. Med. Chem.*, **13**, 2423–2430.
40. Mergny,J.-L. and Hélène,C. (1998) G-quadruplex DNA: a target for drug design. *Nature Med.*, **4**, 1366–1367.
41. Shi,D.F., Wheelhouse,R.T., Sun,D. and Hurley,L.H. (2001) Quadruplex-interactive agents as telomerase inhibitors: synthesis of porphyrins and structure-activity relationship for the inhibition of telomerase. *J. Med. Chem.*, **44**, 4509–4523.
42. Han,H., Langley,D.R., Rangan,A. and Hurley,L.H. (2001) Selective interactions of cationic porphyrins with G-quadruplex structures. *J. Am. Chem. Soc.*, **123**, 8902–8913.
43. Grand,C.L., Han,H., Munoz,R.M., Weitman,S., Von Hoff,D.D., Hurley,L.H. and Bearss,D.J. (2002) The cationic porphyrin TMPyP4 down-regulates c-MYC and human telomerase reverse transcriptase expression and inhibits tumor growth *in vivo*. *Mol. Cancer Ther.*, **1**, 565–73.
44. Cheong,C. and Moore,P.B. (1992) Solution structure of an unusually stable RNA tetraplex containing G- and U-quartet structures. *Biochemistry*, **31**, 8406–8414.
45. Oliver,A.W. and Kneale,G.G. (1999) Structural characterization of DNA and RNA sequences recognized by the gene 5 protein of bacteriophage fd. *Biochem. J.*, **339**, 525–531.
46. Hardin,C.C., Watson,T., Corregan,M. and Bailey,C. (1992) Cation-dependent transition between the quadruplex and Watson–Crick hairpin forms of d(CGCG3GCG). *Biochemistry*, **31**, 833–841.
47. Seenisamy,J., Rezler,E.M., Powell,T.J., Tye,D., Gokhale,V., Sharma Joshi,C., Siddiqui-Jain,A. and Hurley,L.H. (2004) The dynamic character of the G-quadruplex element in the c-MYC promoter and modifications by TMPyP4. *J. Am. Chem. Soc.*, **126**, 8702–8707.
48. Michelotti,E., Tomonaga,T., Krutzsch,H. and Levens,D. (1995) Cellular nucleic acid binding protein regulates the CT element of the humna c-myc protooncogene. *J. Biol. Chem.*, **270**, 9494–9499.
49. Ritchie,S.A., Pasha,M.K., Batten,D.J., Sharma,R.K., Olson,D.J., Ross,A.R. and Bonham,K. (2003) Identification of the SRC pyrimidine-binding protein (SPy) as hnRNP K: implications in the regulation of SRC1A transcription. *Nucleic Acids Res.*, **31**, 1502–1513.
50. Michelotti,E.F., Michelotti,G.A., Aronsohn,A.I. and Levens,D. (1996) Heterogeneous nuclear ribonucleoprotein K is a transcription factor. *Mol. Cell. Biol.*, **16**, 2350–2360.
51. Hildebrandt,M., Lacombe,M.L., Mesnildrey,S. and Veron,M. (1995) A human NDP-kinase B specifically binds single-stranded poly-pyrimidine sequences. *Nucleic Acids Res.*, **23**, 3858–3864.